

Evaluation of a luminometric cell counting system in context of antimicrobial photodynamic inactivation

Moritz Lehnig, Sarah Glass, Norman Lippmann, Svitlana
Ziganshyna, Volker Eulenburg, Robert Werdehausen

Angaben zur Veröffentlichung / Publication details:

Lehnig, Moritz, Sarah Glass, Norman Lippmann, Svitlana Ziganshyna, Volker Eulenburg, and Robert Werdehausen. 2022. "Evaluation of a luminometric cell counting system in context of antimicrobial photodynamic inactivation." *Microorganisms* 10 (5): 950. <https://doi.org/10.3390/microorganisms10050950>.



Article

Evaluation of a Luminometric Cell Counting System in Context of Antimicrobial Photodynamic Inactivation

Moritz Lehnig¹, Sarah Glass^{2,†}, Norman Lippmann³, Svitlana Ziganshyna¹, Volker Eulenburg^{1,*} and Robert Werdehausen^{1,*}

¹ Department of Anaesthesiology and Intensive Care, Medical Faculty, University of Leipzig, 04103 Leipzig, Germany; moritz.lehnig@medizin.uni-leipzig.de (M.L.); svitlana.ziganshyna@medizin.uni-leipzig.de (S.Z.)

² Leibniz Institute of Surface Engineering (IOM), 04318 Leipzig, Germany; sarah.glass@hereon.de

³ Institute for Medical Microbiology and Epidemiology of Infectious Diseases, University of Leipzig, 04103 Leipzig, Germany; norman.lippmann@medizin.uni-leipzig.de

* Correspondence: volker.eulenburg@medizin.uni-leipzig.de (V.E.); robert.werdehausen@medizin.uni-leipzig.de (R.W.)

† Current Address: Helmholtz-Zentrum Hereon, Institute of Membrane Research, 21502 Geesthacht, Germany.

‡ These authors contributed equally to this work.



Citation: Lehnig, M.; Glass, S.; Lippmann, N.; Ziganshyna, S.; Eulenburg, V.; Werdehausen, R. Evaluation of a Luminometric Cell Counting System in Context of Antimicrobial Photodynamic Inactivation. *Microorganisms* **2022**, *10*, 950. <https://doi.org/10.3390/microorganisms10050950>

Academic Editor: Adelaide Almeida

Received: 30 March 2022

Accepted: 28 April 2022

Published: 30 April 2022

Publisher's Note: MDPI stays neutral with regard to jurisdictional claims in published maps and institutional affiliations.



Copyright: © 2022 by the authors. Licensee MDPI, Basel, Switzerland. This article is an open access article distributed under the terms and conditions of the Creative Commons Attribution (CC BY) license (<https://creativecommons.org/licenses/by/4.0/>).

Abstract: Antimicrobial resistance belongs to the most demanding medical challenges, and antimicrobial photodynamic inactivation (aPDI) is considered a promising alternative to classical antibiotics. However, the pharmacologic characterization of novel compounds suitable for aPDI is a tedious and time-consuming task that usually requires preparation of bacterial cultures and counting of bacterial colonies. In this study, we established and utilized a luminescence-based microbial cell viability assay to analyze the aPDI effects of two porphyrin-based photosensitizers (TMPyP and THPTS) on several bacterial strains with antimicrobial resistance. We demonstrate that after adaptation of the protocol and initial calibration to every specific bacterial strain and photosensitizer, the luminometric method can be used to reliably quantify aPDI effects in most of the analyzed bacterial strains. The interference of photosensitizers with the luminometric readout and the bioluminescence of some bacterial strains were identified as possible confounders. Using this method, we could confirm the susceptibility of several bacterial strains to photodynamic treatment, including extensively drug-resistant pathogens (XDR). In contrast to the conventional culture-based determination of bacterial density, the luminometric assay allowed for a much more time-effective analysis of various treatment conditions. We recommend this luminometric method for high-throughput tasks requiring measurements of bacterial viability in the context of photodynamic treatment approaches.

Keywords: photodynamic therapy; photodynamic inactivation; luminescence measurement; antimicrobial resistance; TMPyP; THPTS

1. Introduction

The increasing occurrence of antibiotic resistance in bacteria is a major clinical challenge. Despite intense research, only very few new antibiotics with a novel mechanism of action have been identified [1,2]. Therefore, new strategies that do not depend on specific bacterial structures, such as antimicrobial photodynamic inactivation (aPDI), constitute highly interesting alternatives [3–5]. In PDI, a non-toxic photosensitizer binds to or is taken up by the bacteria [6]. For aPDI, porphyrin-based sensitizers are currently evaluated most often [5], but there is a broad range of other naturally occurring as well as synthetic compounds with photosensitizing properties [3,7], including quinone derivatives, phenothiazines such as methylene blue, and xanthenes, including phthaleins and fluorescein derivatives such as *Rose Bengal*. Upon illumination, these sensitizers induce the generation

of reactive oxygen species (ROS), such as singlet oxygen [8,9], that can inactivate bacteria in a variety of ways [10,11] and independently of possible antibiotic resistances [7].

Ongoing research focuses on further optimization of photosensitizers for specific applications [12,13], as well as on the in-detail characterization and comparison of different photosensitizers in vitro [14–16]. Additionally, photosensitizers were tested in in vivo models for critical infections [17–19]. Unfortunately, the assessment of one central readout in these experiments, the number of viable bacteria, is labor-intensive and time-consuming, which limits the amount of processable samples. Therefore, a scalable approach that allows for the parallel analysis of various treatment conditions and a great variety of different pathogens that are clinically relevant is urgently required.

In this study, we aimed to establish a reliable, fast and scalable method for the detection of viable bacteria with a faster processing time and limited manual manipulation, as compared to standard processes that involve agar plate cultures and the counting of bacterial colonies formed after incubation [20,21]. Previously described methods with higher throughput, such as the antibody-based Raman technique for multiplex optical quantification, do require sophisticated and expensive equipment [22], and PCR methods cannot discriminate between inactivated and viable bacteria [23]. Thus, we used a chemiluminescence-based cell viability system that enables the detection of ATP-dependent luminescence in a 96-well format as a surrogate for the number of viable bacteria in solution. This system is based on firefly luciferin, which is catalyzed by recombinant luciferase in the presence of magnesium (Mg^{2+}) ions, ATP and molecular oxygen. This mono-oxygenation of luciferin is a chemically exothermic reaction that results in oxyluciferin, adenosine monophosphate (AMP), inorganic pyrophosphate, carbon dioxide (CO_2) and yellow-green (550–570 nm) light emission [24]. Therefore, the amount of ATP contained in the sample to be analyzed can be inferred from the amount of light measured [25].

For the evaluation of the modified luminescence-based method, we selected the porphyrin-based photosensitizers TMPyP and THPTS, which are both cationic and water-soluble [5,13] but differ in their optical properties and require different light activation.

We investigated the photodynamic inactivation of several bacterial strains, including Gram-positive *Staphylococcus aureus* and *Enterococcus faecium* and Gram-negative bacteria such as *Escherichia coli*, *Klebsiella pneumoniae*, *Actinobacter baumannii*, *Pseudomonas aeruginosa*, *Achromobacter xylosoxidans* and *Morganella morganii*. For all of these pathogens, antimicrobial resistances (AMR) have been described that are a serious threat and a great challenge to the global public health today [1].

2. Materials and Methods

2.1. Bacterial Strains and Growth Media

All investigated bacterial strains are listed in Table 1. Individual patient-derived strains were identified by MALDI-TOF mass spectrometry (VITEK-MS, bioMérieux, Marcy-l'Étoile, France) in accordance to Tanis et al. [26]. Antibiotic resistances were tested according to the ISO 20776-1 microbroth dilution method.

Blood agar containing Columbia Blood Agar Base (Oxid, Wesel, Germany) with 5% sheep blood (Fiebig, Idstein-Niederauroff, Germany), 2xYT (Trypton, Yeast, NaCl) and brain–heart infusion (BHI; Oxid) dissolved in 0.9% NaCl solution were used as growth media.

2.2. Culture Conditions

The bacteria were cultured at 37 °C and 5% CO_2 on blood agar plates overnight. Individual colonies were diluted in 0.9% NaCl solution to an initial bacterial density that was optically equivalent to McFarland standard no. 1, corresponding to a concentration of approx. 3×10^8 colony-forming units (CFU)/mL. The resuspended bacteria were diluted to a final concentration of 7.5×10^7 CFU/mL in 0.9% NaCl solution containing 50% BHI and a photosensitizer at the indicated concentrations.

For the detection of viable bacteria by luminescence measurement, PDI-treated bacterial suspensions were incubated in the 24-well plate used for PDI at 37 °C and 5% CO₂ for 90 min and stored at −80 °C (<12 h) until detection.

2.3. Assessment of Bacterial Viability

Quantification of ATP was performed by commercially available luciferase-based assay system (BacTiter-Glo™ Microbial Cell Viability Assay, Promega, Madison, WI, USA). Light signals were detected by a luminescence microplate reader (Berthold Technologies, Centro LB 960, Bad Wildbad, Germany) in non-transparent white 96-microwell plates (Thermo Scientific, Waltham, MI, USA) and analyzed by Microwin 2010 software (version 5.17, Mikrotek Laborsysteme GmbH, Neunkirchen-Seelscheid, Germany). Samples (50 µL) were measured in duplicates with a registration time of 1 s per well. Luminescence data are presented as raw RLU data detected after incubation without any adaptation.

For classic clonogenic bacterial density quantification immediately after aPDI, 100 µL of bacterial suspension was diluted by a factor of 10^{−3} to 10^{−6} in 0.9% NaCl solution in order to achieve a high counting accuracy, then spread out with a Drigalski spatula on blood agar plates and incubated for 20 h ± 4 h at 37 °C and 5% CO₂. Subsequently, the agar plates were photographed, and the colony numbers were counted using Image J (Rasband, W.S., U.S. National Institutes of Health, Bethesda, MD, USA) to determine the colony-forming units (CFU). In contrast to other bacterial strains, *Achromobacter xylosoxidans* required 48 h of incubation at 37 °C and 5% CO₂ in order to ensure sufficient visibility of colonies.

2.4. Photodynamic Treatment

The photosensitizer TMPyP 4,4',4'',4'''-(5,10,15,20-tetrayl)tetrakis(1-methylpyridin-1-ium)porphyrin tetratosylate was purchased in the highest available purity (97%) (Product 323497, Sigma Aldrich Chemistry GmbH, Steinheim, Germany). The photosensitizer THPTS (3,3',3'',3'''-(7,8,17,18-tetrahydro-21H,23H-porphyrine-5,10,15,20-tetrayl) tetrakis[1-methyl-pyridinium] tetratosylate, purity 95%), characterized in other studies [27,28], was purchased from TetraPDT GmbH (Rackwitz, Germany).

Illumination was performed in transparent 24-well plates (Cellstar, Greiner bio-one, Frickenhausen, Germany). For TMPyP, we used a custom-made planar LED array-based illumination device, previously analyzed by Habermann et al. [29], with an intensity maximum of 13 mW/cm² at λ_{cent} = 420 nm at a distance of 8 cm. This setup enabled a homogenous light application of all samples on the microwell plate.

For THPTS illumination, a custom-made planar LED array (LEDs: SMB1N 760d, Roitner Laser, Vienna, Austria) with an intensity maximum of 18 mW/cm² at λ_{cent} = 760 nm at a distance of 8 cm was used. A power supply (Bio Rad, Power Pac HC, Hercules, CA, USA) was used to power this light source. Light intensity was measured with a power meter (FieldMax2 TP, Coherent, Portland, OR, USA).

Both photosensitizers were prepared and stored in stock solutions (0.8 mM in 0.9% NaCl) in the dark at 4 °C for a maximum of three weeks before use. For photodynamic treatment, the photosensitizer stock solution was added to the bacterial suspensions to obtain the final concentrations indicated (0 to 200 µM). aPDI was performed at a volume of 1 mL per well.

After the addition of the photosensitizer, all samples were preincubated for 20 min. For TMPyP-treated samples, illumination was started for 0, 60, 90 and 120 min, as previously described [30,31]. For THPTS-based aPDI treatment, bacteria were illuminated for 0, 4, 12, 36 and 108 min in accordance with Ziganshyna et al. [32]. Additional samples were stored under identical conditions but protected from light (dark control). After light exposition, the samples were protected from light and subjected to luminometric cell counting or culture-based determination of bacterial density.

Table 1. Classification of bacterial strains by Gram-stain and antibiotic resistance.

Classification	Gram-Stain	Resistances [33]
<i>Escherichia coli</i>	negative	Extended spectrum beta-lactamase (ESBL)
<i>Staphylococcus aureus</i>	positive	Methicillin-resistant (MRSA)
<i>Klebsiella pneumoniae</i>	negative	ESBL-producing, fluoroquinolone-resistant, carbapenem-resistant (CRE)
<i>Acinetobacter baumannii</i>	negative	Extensively drug-resistant (XDR)
<i>Enterococcus faecium</i>	positive	Vancomycin-resistant (VRE)
<i>Pseudomonas aeruginosa</i>	negative	Multidrug-resistant (MDR) (including carbapenems)
<i>Morganella morganii</i>	negative	-
<i>Achromobacter xylosoxidans</i>	negative	Extensively drug-resistant (XDR)

2.5. Spectrometry

The absorption spectrometry of photosensitizers and bacterial growth media, as well as the luminescence spectrometry of the Cell Viability Assay, was performed with a SpectraMax M5 instrument (Molecular Devices, San José, CA, USA).

2.6. Statistical Analysis

Data are presented as mean \pm SD. Differences between groups were determined using one- or two-way ANOVA and Bonferroni post hoc test. For cross-correlation analysis, corresponding value pairs determined by the two different detection methods were plotted against each other to assess a linear correlation. Calculations were performed with GraphPad Prism (version 7.0, GraphPad, San Diego, CA, USA).

3. Results

3.1. Evaluation of a Luminescence-Based Approach for the Determination of aPDI Effects

To test whether a luminometric quantification of ATP in bacterial lysates after aPDI treatment was suitable for the determination of the aPDI effects on bacterial growth, we determined the effect of 0 to 200 μ M TMPyP and illumination for 0 to 120 min with 13 mW/cm² at λ_{cent} 420 nm on *E. coli* using conventional bacterial culture and colony counting. Consistent with previous results, we found a reduction in the bacterial colony number [34], which depended on the photosensitizer concentration and illumination time (Figure 1A,B).

When we analyzed the bacterial viability as determined by the ATP concentration in bacterial cell lysates after aPDI treatment following the manufacturer's instructions, we observed a clear reduction in the luminescence in bacterial lysates after aPDI treatment, as compared to lysates that were only incubated with the photosensitizer but that were protected from light, suggesting that the aPDI effects can be determined using this approach. However, the addition of only the photosensitizer (without any illumination) also caused a significant reduction in detected luminescence, suggesting that the photosensitizer interferes with the assay system (Figure 1C). Therefore, we decided to develop an adapted protocol by performing additional preliminary experiments.

To determine whether the optical properties of the photosensitizers interfere with the luminescence measurement, we determined the absorption spectrum of TMPyP dissolved in 50% BHI-NaCl solution. Consistent with the optimal wavelength for aPDI treatment, the absorption maximum was detected at $\lambda = 428$ nm. The absorption of the 50% BHI medium itself continually decreases at wavelengths higher than 320 nm. At $\lambda = 428$ nm, the absorption declines below 0.52 arbitrary units. To determine possible interference with the luminescence detection assay system, the emission spectrum of the used luciferase was determined. Here, the highest intensity of the emitted light was detected at $\lambda \approx 556$ nm, with significant intensities being observed in the range from 480 nm to 730 nm. These data indicated that there is no overlap between the main absorption maximum of TMPyP and the assay-induced luminescence. Nevertheless, there was an increased

optical density of the solution from $\lambda = 480$ to 730 nm (Figure 1D). To test whether TMPyP interferes with the detection of luciferase-emitted luminescence, we determined the ATP-induced luminescence in our assay system in the presence of increasing concentrations of TMPyP. Indeed, a dose-dependent reduction in the apparent luminescence was observed (Figure 1E). To test whether this was due to the optical properties of TMPyP or due to the direct interference of TMPyP with the luciferase or any other component of the detection system, we determined the luminescence elicited by different ATP concentrations in the presence or absence of TMPyP. Here, in all samples, a constantly decreased luminescence by $67.9\% \pm 3.3\%$ ($n = 4$) in the presence of TMPyP was observed (Figure 1F), demonstrating that TMPyP functions as a quencher for luciferase-emitted luminescence without directly interfering with the detection system. To compensate for this quenching, in all subsequent experiments, the TMPyP concentration was adjusted to the highest concentration used in the respective experiment prior to luminescence measurements.

Next, we investigated whether TMPyP itself had any direct influence on the ATP metabolism of the bacteria or any effect on the lysis efficacy prior to the luminescence detection. Therefore, we performed the bacterial lysis of Gram-negative *Escherichia coli* before and after TMPyP addition and compared the assay-induced luminescence. At a concentration of 200 μM TMPyP, representing the highest used concentration during photodynamic treatment, no relevant influence on the luminescence of the assay and the associated ATP release was observed (Figure 1G).

Since ATP content is used for the luminometric detection of viable bacteria, which is dependent on bacterial metabolism, we assumed that the time between aPDI treatment and bacterial lysis was a critical variable. Here, a comparison of the luminescence elicited by lysates from heat-inactivated *E. coli* to that from viable bacteria revealed a time-dependent increase in the difference in luminescence compared to the control group (Figure 1H). Similar findings resulted from experiments with extensively drug-resistant (XDR) *Achromobacter xylosoxidans*, Vancomycin-resistant Enterobacteriaceae (VRE) *Enterococcus faecium*, multidrug-resistant (MDR) *Pseudomonas aeruginosa* and XDR *Acinetobacter baumannii* (Figure S1).

Another source of error to be considered was the background luminescence of the luciferase-based assay, which is influenced by the type of bacterial growth medium because of the luminescence-inducing ATP in their ingredients. Regarding our aPDI experiments, two growth media were compared. A 17.5 times lower background luminescence of 4436 ± 88.6 RLU was observed in the BHI bacterial growth medium compared to $775,434 \pm 1399.6$ RLU in the 2xYT growth medium (Figure S2A).

Based on these findings, we implemented the following adjustments to the protocol for luminescence-based determination: First, the TMPyP concentration of all bacterial lysates was adjusted to the highest concentration in the respective experiment. Second, all samples were incubated for 90 min after the aPDI treatment before luminescence detection. With these optimizations, we again determined the aPDI effect caused by 200 μM TMPyP on *E. coli* in comparison to samples that were only illuminated without TMPyP (light control) or only treated with the photosensitizer without illumination (dark control) (Figure 1I). The relative reduction in luminescence in the dark control by $26.5\% \pm 5.2\%$ were now similar to the relative reduction observed with the conventional colony-counting method (by $24.2 \pm 7.5\%$; Figure 1B). Moreover, a significant aPDI effect was detected by the reduction in luminescence (by $91.0\% \pm 0.2\%$, Figure 1I) and by the reduction in the counted colony number by $99.2\% \pm 0.1\%$ (Figure 1B).

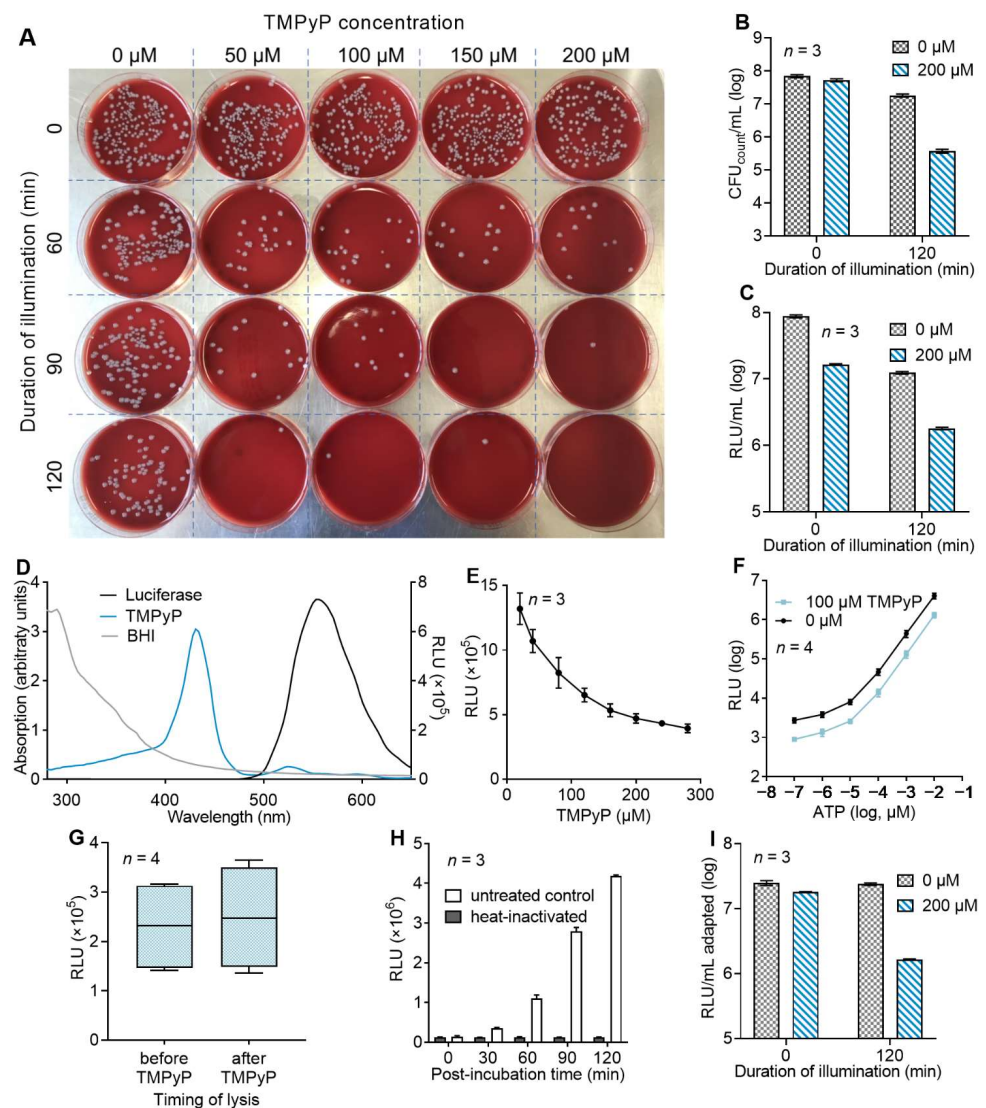


Figure 1. ATP-based luminometry as a novel approach to measure aPDI effects in vitro. (A) *E. coli* bacteria were treated with TMPyP at the indicated concentration and exposed to light (13 mW/cm^2 at $\lambda_{\text{cent}} = 420 \text{ nm}$; 0.78 J/cm^2 per minute) for the indicated durations. Bacteria were spread on blood agar plates (dilution factor 10^{-5}) and incubated for 20 h (37°C , $5\% \text{ CO}_2$). (B) aPDI effect of the experiment described in A without or with $200 \mu\text{M}$ TMPyP determined as $\text{CFU}_{\text{count}}/\text{mL}$. (C) *E. coli* were incubated without or with $200 \mu\text{M}$ TMPyP and treated for 0 or 120 min with light as described in A. Bacterial viability was determined by ATP-induced luminescence in bacterial lysates. (D) Absorption spectrum of $40 \mu\text{M}$ TMPyP dissolved in 50% BHI bacterial growth medium dissolved in 0.9% NaCl solution. Additionally, the luminescence spectrum of the luciferase used in the cell viability assay and absorption spectrum of the BHI medium are displayed. (E) Effect of different TMPyP concentration on ATP-induced luminescence; TMPyP at indicated concentrations was supplemented with 5 nM ATP (in 0.9% NaCl solution) and ATP-induced luminescence was determined ($n = 3$). (F) Luminescence elicited by ATP at the indicated concentrations (in 0.9% NaCl) in the presence or absence of $100 \mu\text{M}$ TMPyP ($n = 4$). (G) Effect of TMPyP on bacterial ATP metabolism. *E. coli* suspended in 50% BHI were lysed before or after addition of $200 \mu\text{M}$ TMPyP ($n = 4$). (H) *E. coli* suspended in 50% BHI broad medium were heat-inactivated or left untreated and incubated at 37°C , $5\% \text{ CO}_2$ in the same solution as active bacteria for the indicated duration. Bacteria were lysed, and luminescence was measured with the cell viability assay ($n = 3$). (I) aPDI effect of the experiment described in C with $200 \mu\text{M}$ TMPyP, measured 90 min after incubation (37°C , $5\% \text{ CO}_2$) and adjusted to highest PS concentration ($200 \mu\text{M}$) in all samples prior to measurements.

3.2. Correlation of Results for Density of Viable Bacteria Determined by Luminescence or Conventional Colony Counting

To allow for a direct comparison of the ATP concentration within the lysates as determined by the luminometric measurement with the number of bacteria found in a given sample, we developed a standardized protocol that allowed for the conversion of the detected luminescence (RLU) to the corresponding and more conventional measuring unit CFU/mL.

To this end, the corresponding values from both detection types of *E. coli* were compared at three different incubation times ($t = 0, 120, 210$ min) and, therefore, at increasing densities. This enabled us to determine the bacterial growth rate (R) and the resulting ATP concentration in a bacterial solution under these conditions (Figure 2A). The bacterial growth rate (R) was defined as the logarithm of the $RLU_{210 \text{ min}}$ value to the base of the $RLU_{120 \text{ min}}$ value, assuming exponential growth. Additionally, we assumed that the luminescence detected in the lysates of heat-inactivated bacteria equaled a bacterial density of zero.

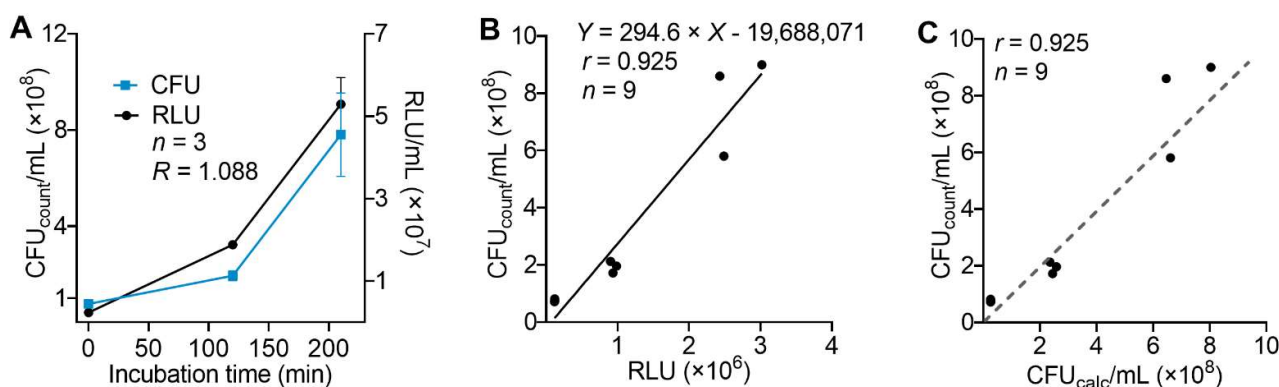


Figure 2. Correlation of luminescence-based readout and bacterial density as determined by colony counting. (A) *E. coli* suspended in 50% BHI broad medium were incubated at 37 °C, 5% CO₂, and CFU_{count}/mL were determined by spreading aliquots on agar plates and counting bacterial colonies after 20 h. In parallel, bacterial density was determined on the basis of ATP-dependent luminescence in bacterial lysates. The bacterial growth rate (R) was defined as the logarithm of RLU_{210} to the base of RLU_{120} , assuming exponential growth (similar to that obtained on basis of CFU_{count}). (B) Linear correlation between luminescence values as relative luminescence units (RLU) and bacterial density determined as CFU_{count}/mL. Luminescence detected in bacterial lysates from samples heat-inactivated at $t = 0$ min were set to zero CFU/mL. (C) Comparability of recalculated bacterial density (CFU_{calc}/mL) to manually counted bacterial density (CFU_{count}/mL) of ESBL *E. coli*.

To calculate bacterial density in aPDI experiments after incubation, the detected raw RLU data had to be adapted before further calculation, accounting for the bacterial growth rate (R): $RLU_{adapt} = (RLU_{PDI})^{1/R}$.

The corresponding data from both detection methods were then used for linear regression analysis (Figure 2B), which allowed us to convert RLU data to calculated CFU_{calc}/mL with a good correlation for TMPyP-based aPDI and *E. coli* bacteria ($r = 0.925$, Figure 2C).

3.3. Standard Protocol to Establish Luminescence-Based Cell Density Determination for aPDI Experiments with Other Photosensitizers and Bacterial Strains

Taken together, we propose the following steps to determine calibration factors when performing aPDI experiments with new bacterial strains and/or other aPDI conditions, such as, for example, a novel photosensitizer. Our aPDI treatment protocol (Figure 3) consists of 20 min preincubation of samples with the photosensitizer, followed by illumination as described in the respective aPDI protocol. The post-aPDI incubation period was standardized to 90 min. Control samples without PS and illumination are mandatory. As

described above, the photosensitizer concentration in all samples must be adjusted to the maximum concentration used in the experiment prior to luminometric measurements.

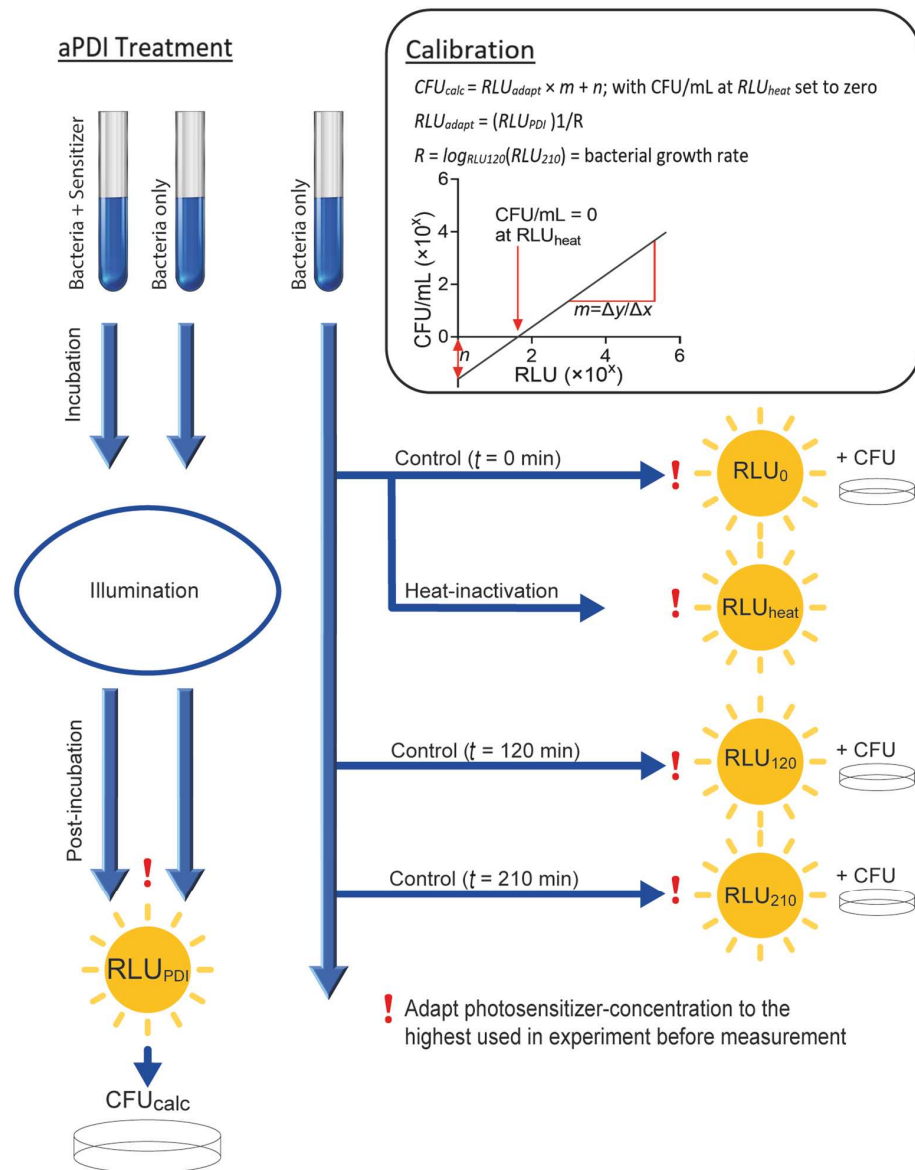


Figure 3. A schematic presentation of the standard procedure for determining aPDI effects with a given photosensitizer on any bacterial strain. The required calibrations to correlate the luminescence reading to previously determined colony-forming units (CFU) are illustrated. In order to calculate bacterial density (CFU_{calc}) from luminescence values, a regression analysis of corresponding data pairs from control group experiments is required. Corresponding values before illumination, after complete illumination and after post-incubation enable a linear regression analysis between luminescence and bacterial density. Additionally, the bacteria-specific replication time (R) was determined by this measurement and used to calculate the bacterial density after aPDI. The luminescence observed in samples from heat-inactivated bacteria was defined as the luminescence emitted at a density of zero CFU/mL for viable bacteria. Process of calculation after calibration: 1. Determine bacterial growth rate (R) = $\log_{RLU(120min)} RLU(210min)$; 2. Calculate bacterial density in RLU ($RLU_{adapt} = RLU_{PDI}^{1/R}$); 3. Use RLU_{adapt} to calculate CFU_{calc}/mL by linear regression, set to zero CFU/mL at luminescence of heat-inactivated bacteria according to the formula $CFU_{calc}/mL = RLU_{adapt}/mL \times m + n$ with m and n derived from linear regression-fitting results; 4. Define calculated data less than or equal to zero as zero CFU/mL.

The correlation factors between luminescence intensity (in RLU) and bacterial density (in CFU_{count}/mL) are determined by analyzing the untreated bacterial samples ($n = 3$) using both methods after incubation times of $t = 0, 120, 210$ min (corresponding to the incubation times used in the aPDI experiments). Additionally, heat-inactivated samples of the control ($t = 0$ min) are measured in order to determine the luminescence that is detected at a bacterial density of zero. The bacterial growth rate (R) was determined between 120 min and 210 min (corresponding to 90 min post-incubation). This enables a calculation of the bacterial density data from the luminescence data directly after treatment (120 min), using the luminescence data detected after incubation (210 min).

The observed comparability between luminescence intensity (RLU) and bacterial density (CFU_{count}/mL) in the controls ($n = 3$) then allows for the calculation of bacterial density (CFU_{calc}/mL) from aPDI data, according to the following equation (and Figure 3):

$$R = \log_{RLU(120\text{min})} RLU(210\text{min}) = \text{bacterial growth rate}$$

$$RLU_{adapt} = (RLU_{PDI})^{1/R}$$

$$CFU_{calc} = RLU_{adapt} \times m + n$$

3.4. Evaluation of the Luminescence-Based Assay Protocol with Different Bacterial Strains in the Context of aPDI

Subsequently, the above-established protocol was used to analyze the aPDI effects of TMPyP on different clinically relevant patient-derived bacterial strains. To obtain the required bacterial growth rate and conversion factors for the individual bacterial strains used, samples were prepared and analyzed in accordance with Section 2.3 and Figure 3. For most bacterial strains tested in this study, the protocol led to a good correlation between luminometric registrations and manually counted colonies. Here, in the Gram-negative extended spectrum beta-lactamase (ESBL) *Escherichia coli*, which were used to establish the protocol, we found an aPDI-induced RLU decrease of $89.6\% \pm 3.1\%$ with 200 μM TMPyP and an illumination time of 120 min (Figure 4A). This corresponds to a calculated reduction in bacterial density (CFU_{calc}) of $95.5\% \pm 4.8\%$ (Figure 4B). Conventional colony counting resulted in a reduction in bacterial density of $99.9\% \pm 0.1\%$ (Figure 4D) after aPDI treatment. A correlation analysis between the two methods for bacterial density measurement revealed a correlation coefficient of $r = 0.762$ ($p < 0.0001$, Figure 4C). This result indicates that the aPDI effects on *E. coli* are slightly underestimated when assessed with the luminescence method.

To extend our experiments to other Gram-negative bacterial strains not previously analyzed, we analyzed the effect of TMPyP-elicited aPDI effects on XDR *Acinetobacter baumannii*. Here, we observed a blue-light susceptibility that was independent from TMPyP, which caused a reduction in luminescence after 120 min illumination of $96.0 \pm 2.0\%$ (Figure 4E). This resulted in a calculated CFU reduction of $88.4 \pm 2.7\%$, which could not be further increased with 200 μM TMPyP (reduced by $90.5 \pm 1.1\%$, Figure 4F). This result correlated well with the counted bacterial density, which was reduced by $92.5 \pm 8.6\%$ under 120 min illumination without TMPyP ($r = 0.719$; $p < 0.0001$, Figure 4G) and reduced by $99.8 \pm 0.2\%$ with 200 μM TMPyP (Figure 4H). Again, the effects of aPDI were underestimated with the luminometric method.

For VRE *Enterococcus faecium*, which has previously shown a high susceptibility to TMPyP treatment already at the lowest concentration investigated (50 μM , 60 min illumination), we observed a reduction in luminescence of $93.1 \pm 1.9\%$ (Figure 4I). Here, our calculation method resulted in a bacterial density less than zero (Figure 4J). These findings indicate an increased scattering between calculated and manually detected values and a lower sensitivity of the luminescence method at low bacterial densities ($r = 0.236$, $n = 38$, $p = 0.1531$, Figure 4K). The susceptibility of VRE *Enterococcus faecium* to TMPyP-based aPDI was confirmed by manually determined bacterial density (reduction of $99.99 \pm 0.02\%$; Figure 4L), thereby confirming the finding of our previous study [34].

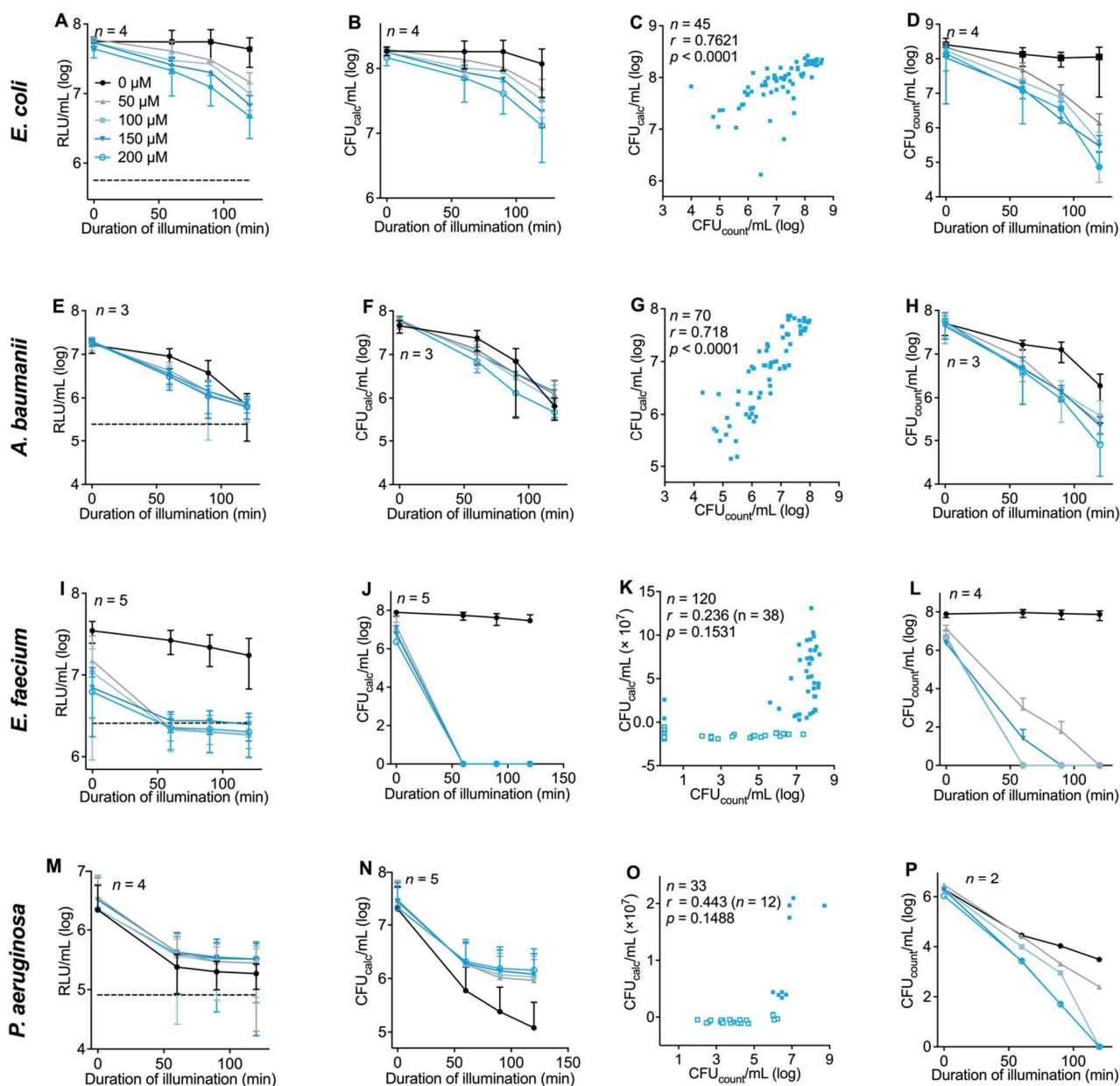


Figure 4. Evaluation of aPDI effects of TMPyP on different bacterial strain as determined by ATP-evoked luminescence and manual counting of bacteria colonies. Data from the aPDI experiments are presented. TMPyP at indicated concentrations was illuminated with 13 mW/cm^2 resulting in 0 J/cm^2 (0 min), 46.8 J/cm^2 (60 min), 70.2 J/cm^2 (90 min), 93.6 J/cm^2 (120 min) at $\lambda_{\text{cent}} = 420 \text{ nm}$; the dashed line shows the luminescence of heat-inactivated bacteria. (A) ATP-induced luminescence of ESBL *E. coli* after aPDI. (B) Calculated bacterial density (CFU_{calc}) of ESBL *E. coli* based on luminometric measurements. (C) Correlation between CFU_{calc} and manually determined bacterial density ($\text{CFU}_{\text{count}}$) in ESBL *E. coli*; r = correlation coefficient. (D) $\text{CFU}_{\text{count}}$ of viable ESBL *E. coli* after aPDI. (E–H) Results for XDR *A. baumannii* as described above for *E. coli*. (I–L) Results for VRE *E. faecium*; calculated values less the zero were excluded per definition (empty boxes). (M–P) Results for MDR *P. aeruginosa*.

In addition to the pronounced aPDI effect, a dark toxicity of TMPyP was observed in VRE *E. faecium*. To this end, the luminescence detected in samples that were exposed to $200 \mu\text{M}$ TMPyP but kept in the dark was already reduced by $80.6 \pm 3.5\%$ (Figure 4I). To further examine the observed dark toxicity of TMPyP in *E. faecium*, the ATP-induced luminescence was detected before and after incubation with TMPyP ($200 \mu\text{M}$) for 120 min in the dark. In samples treated with TMPyP, the luminescence increased from $11.7 \times 10^4 \pm 0.8 \times 10^4 \text{ RLU}$ to

$35.5 \times 10^4 \pm 4.0 \times 10^4$ RLU, whereas the ATP-induced luminescence of untreated samples increased from $11.2 \times 10^4 \pm 0.8 \times 10^4$ to $66.0 \times 10^4 \pm 0.3 \times 10^4$ RLU (Figure S2B).

Consistent with previous data, MDR *Pseudomonas aeruginosa* revealed a significant background luminescence most likely caused by a pyoverdine-induced luminescence [35] that increases the luminescence of bacteria (Figure 4M). This increased background luminescence hampers the calculation of bacterial density. Consequently, the correlation of the calculated and actually observed density of the bacteria was very poor, especially at lower bacterial densities ($r = 0.443$, $n = 12$, $p = 0.1488$). Calculated values less than zero were excluded from the calculations (Figure 4O). The increased cut-off precluded a distinction of aPDI effects at different TMPyP concentrations (Figure 4N,O). Therefore, bioluminescence of bacterial strains seems to be an exclusion criterion for this method. However, we observed a reduction in bacterial density of $99.8 \pm 0.27\%$ after illumination with blue light without a photosensitizer. With TMPyP-based aPDI, we observed a concentration-dependent effect of up to a complete inactivation at $200 \mu\text{M}$ TMPyP followed by 120 min illumination, confirmed with manual bacteria counting (Figure 4P).

In the following TMPyP-based aPDI experiments with different bacterial strains, we observed an acceptable correlation between the luminescence-based measurements and manual colony counting: Carbapenem-resistant Enterobacteriaceae (CRE) *Klebsiella pneumoniae* ($r = 0.706$; $p < 0.0001$; Figure S3A), MRSA *Staphylococcus aureus* ($r = 0.894$; $p < 0.0001$; Figure S3B), XDR *Achromobacter xylosoxidans* ($r = 0.696$; $p < 0.0001$; Figure S3C). The corresponding data acquired after aPDI with luminescence measurements and manually determined bacterial densities are presented in Figure S3.

3.5. Using the New Protocol for Characterization of aPDI Effects Elicited by Another Photosensitizer

To transfer the protocol for the characterization of aPDI effects to a different photosensitizer, we selected THPTS, which has previously been shown to have significant clinical potential as a photosensitizer that can be activated by near-infrared light. The initial calibration experiments were performed as described above (Figure 3). THPTS has several absorption peaks with a maximum at $\lambda = 760 \text{ nm}$, which is used during aPDI treatment for excitation, but also a further absorption maximum at $\lambda = 516 \text{ nm}$ that partially overlaps with the luminescence spectrum of the luciferase used in our assay (Figure 5A). Evaluation of the photosensitizer-caused quenching factor revealed a reduction in the luciferase-caused luminescence of $52.8 \pm 4.9\%$ in the presence of $200 \mu\text{M}$ THPTS in BHI broad medium (Figure 5B). As described above for the TMPyP experiments, the lysing property of the assay was examined with and without THPTS in *M. morgani* bacteria. No relevant influence of THPTS on lysing effectivity was observed (Figure 5C).

When performing THPTS-based aPDI experiments, a similar reduction in luminescence and manually determined bacterial density was found in VRE *E. faecium* (Figure 5D). As described above for TMPyP, the bacterial growth rate (R) between 108 min and 198 min (corresponds to 90 min incubation after a typical aPDI experiment with THPTS) was established (Figure 5D), and the ATP-elicited luminescence was determined in samples from the corresponding bacterial lysates in the presence of THPTS. Together with data from the manual bacterial density determination ($t = 0, 108, 198 \text{ min}$), a linear regression analysis for the luminescence data was performed. This analysis indicated a good correlation between the data obtained from the luminometric measurements and the observed bacterial density as assessed by classical clonogenic CFU determination in THPTS-based aPDI experiments ($r = 0.944$, $p < 0.0001$, Figure 5E). Taken together, these data demonstrate that luminometric data in the presence of THPTS could be used to calculate bacterial density with acceptable accuracy (Figure 5F).

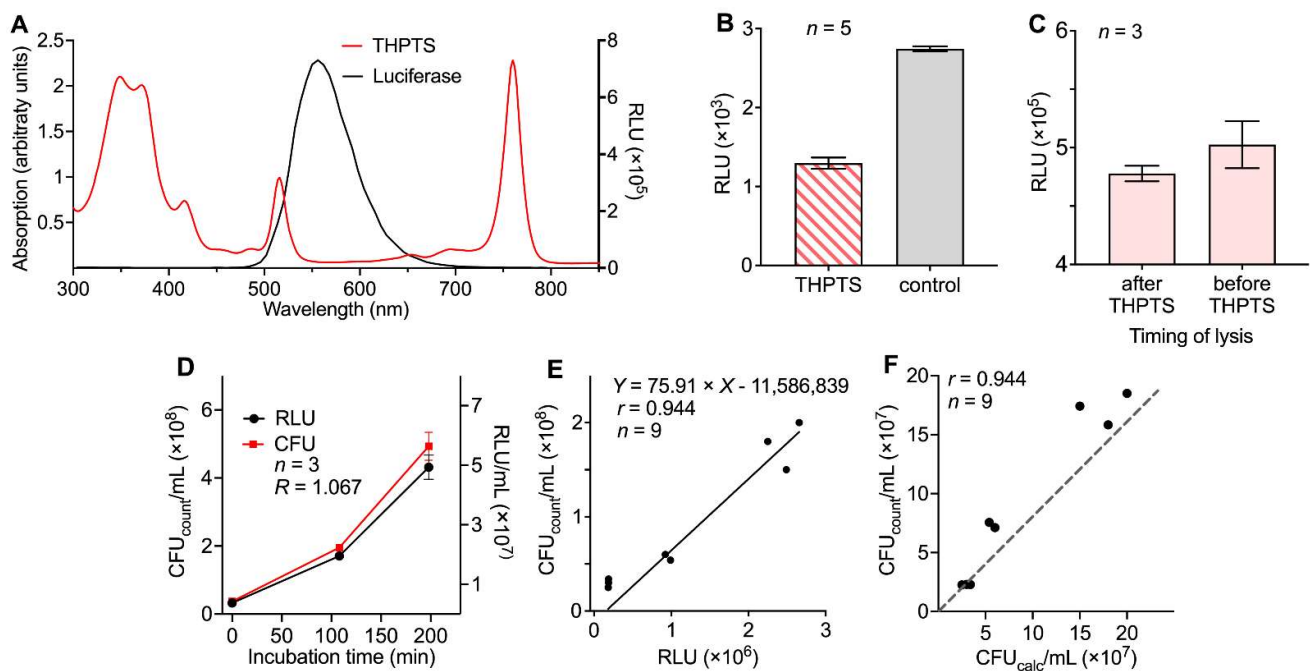


Figure 5. Correlation of bacterial densities as determined by luminescence and manually counting in the presence of the photosensitizer THPTS: (A) The absorption spectrum of THPTS dissolved in 0.9% NaCl was measured. Additionally, the luminescence spectrum of the luciferase used in the cell viability assay is presented. (B) Background luminescence of 50% BHI broad medium (dissolved in 0.9% NaCl) with 200 μ M THPTS compared to 50% BHI broad medium alone. (C) Bacteria-lysing property of the assay was measured with and without THPTS in *M. organii*. (D) Bacterial growth curve of VRE *E. faecium*, incubated in BHI broad medium at 37 $^{\circ}$ C, 5% CO₂, detected at indicated time points. Density of bacteria was determined by luminometric assay and colony counting (CFU_{count}). (E) Correlation between results from luminometric readings and calculated colony density (CFU_{calc}) in VRE *E. faecium*, with results of luminometry in heat-inactivated bacteria used to define zero CFU/mL. (F) Correlation between CFU_{calc} and CFU_{count} of VRE *E. faecium*; r = correlation coefficient.

To identify the aPDI effects of THPTS on VRE *E. faecium* and *M. organii*, the red-light susceptibility or dark toxicity of THPTS was determined. For both bacterial strains, no effect from red light or the photosensitizer alone were observed. VRE *E. faecium* offered, after aPDI, a THPTS concentration-dependent decrease in luminescence, with the greatest reduction of $91.1 \pm 1.5\%$ RLU (200 μ M THPTS; 108 min illumination; Figure 6A). This corresponded to a decreased bacterial density by $81.7 \pm 2.5\%$ CFU_{calc}/mL (Figure 6B). When comparing all calculated and manually counted values for the density of viable bacteria, we observed a correlation of $r = 0.938$ ($p < 0.0001$, Figure 6C). Moreover, analyzing the manually determined values, we found a similar magnitude of density reduction of $92.20 \pm 1.09\%$ (Figure 6D).

For *M. organii*, we observed a reduction in ATP-induced luminescence of $62.5 \pm 0.4\%$ RLU after THPTS-based aPDI (Figure 6E), which resulted in a calculated reduction in bacterial density of $65.6 \pm 0.4\%$ (Figure 6F). Again, there was an acceptable correlation between the calculated and manually observed values for bacterial density ($r = 0.845$; Figure 6G,H).

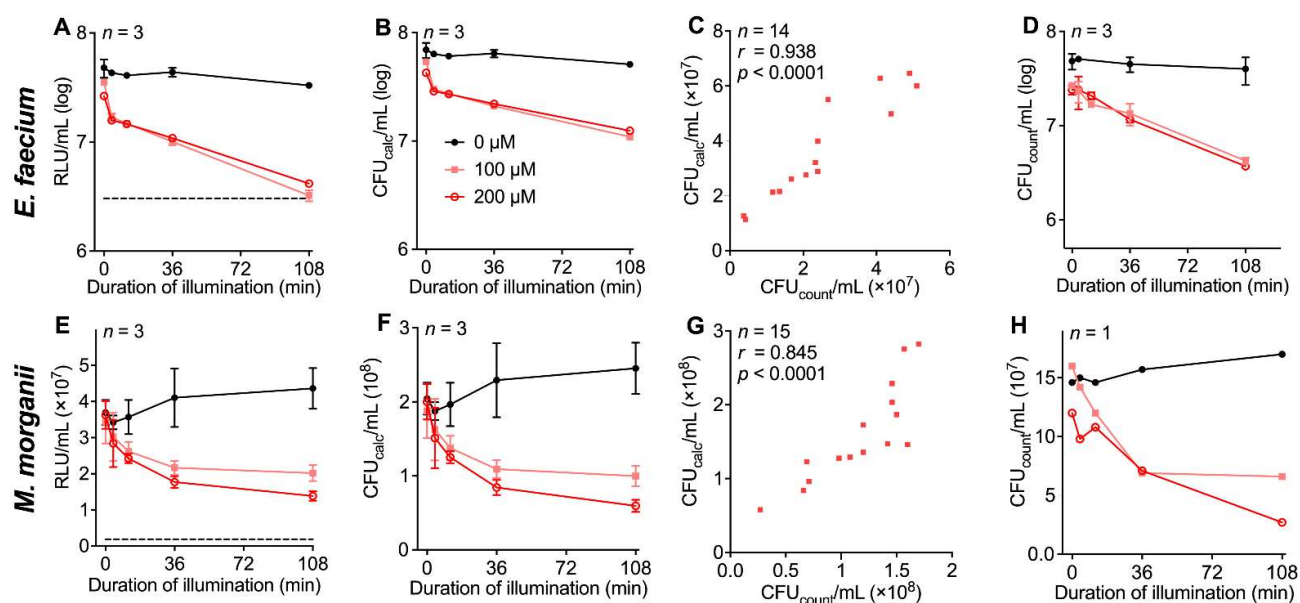


Figure 6. Correlation of calculated and manually detected bacterial density for THPTS-based aPDI in different bacterial types. THPTS was illuminated with 18 mW/cm² resulting in 0 J/cm² (0 min), 4.3 J/cm² (4 min), 12.9 J/cm² (12 min), 38.9 J/cm² (36 min), 116.6 J/cm² (108 min) at $\lambda_{\text{cent}} = 760$ nm. Dashed line indicates the luminescence of heat-inactivated bacteria. (A) ATP-induced luminescence by VRE *E. faecium* after aPDI. (B) Calculated bacterial density of VRE *E. faecium* based on luminometric measurements. (C) Correlation between calculated and manually determined bacterial density in VRE *E. faecium*; r = correlation coefficient. (D) Manually counted bacterial density of VRE *E. faecium* after aPDI. (E–H) Results for *M. morganii* as described above for *E. faecium*.

4. Discussion

To establish a high-throughput method to assess the effects of various aPDI treatments on a great variety of different bacteria, we evaluated the feasibility and limitations of a luminescence-based method, which detects bacterial ATP as a surrogate of bacterial survival.

Although a direct use of the protocols provided by the manufacturer resulted in significant differences in the effect size as determined by the luciferase-based approach and conventional colony counting after preparation of bacterial cultures on agar plates, we were able to establish a protocol that allows for the standardized testing and calibration of the luminescence-based bacterial density measurements and the subsequent comparison of obtained results with previously obtained data from conventional bacterial colony counting.

The feasibility of this approach was shown to depend, on the one hand, on the bacterial strain used, and on the other hand, on the optical properties of the PS. We found that the investigated luminescence-based method is feasible in many of the bacterial strains tested, and the aPDI effects determined by this approach were in good agreement with those obtained by manual counting of bacterial colonies after agar plate culturing [32]. In some bacterial strains, such as MDR *Pseudomonas aeruginosa*, however, the intrinsic properties of the bacteria precluded the use of luminescence-based cell density determination. For other bacterial strains, e.g., *E. coli*, our results demonstrate that a universal conversion of the results obtained by both methods is also not possible. In contrast, individual calibrations are required to account for different types of bacteria, growth media and photosensitizers and, thereby, to minimize the margin of error.

After these initial calibration experiments, the luminescence-based analysis of bacterial viability allowed us to analyze the effects of aPDI with shorter processing times and increased scalability, as compared to the conventional procedure of bacterial cultures and manual colony counting.

Although we considered the clonogenic (growth) method (manual colony counting) as the gold standard for bacterial density detection, we want to emphasize that this method does not allow for the detection of effects that do not lead to a reduced number of colonies but result, e.g., in a slower metabolism, as described by Kramer et al. [36], or in a reduced ability to replicate, which may be caused by aPDI-induced photooxidative DNA damage [37]. Therefore, ATP-based methods may reveal additional facets of the bacteriostatic effects of aPDI [36]. In support of this hypothesis and by using the luminescence method as described here, we could identify a dark toxicity of TMPyP in *E. faecium* that is caused not by a bactericidal but by a bacteriostatic effect, which was not apparent from the conventional colony-counting method. As TMPyP is a positively charged quaternary amine, some antibacterial properties may be expected at concentrations used in our aPDI experiments [38–41].

Using this novel luminescence approach, we could demonstrate the different susceptibilities of several bacterial strains to aPDI. Although aPDI is considered to exert its bactericidal and/or bacteriostatic effect via the generation of ROS, which should affect all bacteria, these variations may result from differences in the accumulation of photosensitizers at the bacterial plasma membrane and other targets of aPDI-induced ROS. Additionally, diverging activities of the repair mechanisms [15,42,43] for ROS-induced damages and/or the systems that mediate the efflux of photosensitizers for the bacteria [44] may contribute to the observed differences in aPDI sensitivity.

Interestingly, in most experiments, the aPDI effect was underestimated by the here-described luminescence-based method as compared to results from colony counting. This may result from a systematic error, since the ATP concentration determined in heat-inactivated bacterial samples at the timepoint $t = 0$ min was defined as the baseline ATP concentration corresponding to a bacterial density of zero in manual counting. In the corresponding aPDI treated samples, the bacteria may still produce significant amounts of ATP before being eliminated by aPDI treatment. It is well-known that photodynamic treatment can change the growing conditions and, subsequently, the ATP synthesis of different bacterial strains in a not-negligible way [36]. Nevertheless, as observed with the high susceptibility of *E. faecium* to TMPyP-based aPDI, the complete inactivation of bacteria could also be verified by the luminometric method. In this bacteria strain, aPDI apparently reduced the ATP concentration to a greater extent than heat inactivation did, which led to the observed negative values for bacterial density as a result of the predefined cut-off based on heat inactivation.

Another critical factor when applying the luminescence method evaluated here is the optimal duration of the post-incubation time of bacterial samples before luminescence detection. Here, optimal results will require an individual testing for each type of bacteria, growing condition and PS. An optimized post-incubation duration may increase the correlation between manual counting and the proposed luminometric method.

Our experiments demonstrated that the optical properties of the PS, as well as the growth media used, may influence the detection of luminescence due to their absorption characteristics. For most components, such as the BHI, this effect was constant and did not change during illumination and could therefore be easily compensated. Absorption properties of other growth media, e.g., blood-containing solutions as well as of some PS, however, may change during aPDI treatment and therefore contribute to the underestimation of aPDI effectivity with the ATP-based luminescence method.

Using the PS THPTS, we tested whether the measurement of the ATP concentration by luminescence detection is suitable to determine the aPDI effect of a given combination of PS and bacteria. Our results indicate that it is possible in most cases to detect the dose-dependent effects of aPDI in detail and for large sample sizes. Combinations that are not suitable for this method, however, must be identified in initial tests beforehand. Moreover, it is necessary to adjust the protocol to specific bacteria and photosensitizers to allow for the comparability of the results obtained by the luminescence method and conventional colony

counting. Some bacterial strains, such as MDR *Pseudomonas aeruginosa*, are not suitable for this approach, in this specific case due to auto-luminescence [35].

Although we could demonstrate that the luminescence method described here is suitable to determine aPDI effects *in vitro*, we cannot judge on its feasibility in samples obtained from *in vivo* aPDI treatments. Here, more adjustments to this method may be required to account for the influence of additional preanalytical confounders, such as the unknown photosensitizer concentration and other contaminants in the samples.

At the time of writing, an ATP-based approach as described here requires assay reagents and disposables of approximately USD 0.25 per sample (not considering probable cost reductions by scaling effects). While the costs of consumables for the classical clonogenic method (preparation of bacterial cultures) may be lower, one should take into account that higher labor costs are likely to arise, at least if manual culture preparation and colony counting are performed.

Based on data from previous studies, the illumination at the indicated doses should be well-tolerated by eukaryotic cells [45–47]. However, our *in vitro* study cannot rule out adverse effects of aPDI in adjacent host tissues.

In conclusion, the evaluated luminescence method is an interesting alternative for the *in vitro* investigation of aPDI effects in many bacterial strains—especially if a high number of samples are to be processed simultaneously, e.g., in order to explore the dose–response relationships of a novel PS or to determine the optimal incubation and illumination times in various bacterial strains. Here, initial calibration experiments are still required to allow for a good agreement of the obtained results to those from the clonogenic method. While the clonogenic method has its own limitations, e.g., strains of bacteria that are difficult to cultivate, it is certainly more robust with regard to the interference of photosensitizers, growth medium and bacterial autofluorescence. Despite these limitations, the measurement of bacterial density by ATP-dependent luminescence provides the basis for a scalable multidimensional approach to assess the aPDI effects of a given bacteria/PS combination.

Supplementary Materials: The following supporting information can be downloaded at: <https://www.mdpi.com/article/10.3390/microorganisms10050950/s1>, Figure S1: Luminescence of heat-inactivated bacteria compared to active bacteria, dependent on post-incubation time, Figure S2: Background luminescence of bacteria growth media and VRE *E. faecium* susceptibility to TMPyP without illumination, Figure S3: Further evaluation of aPDI effects of TMPyP on different bacterial strains as determined by ATP-evoked luminescence and manual counting of bacteria colonies.

Author Contributions: Conceptualization, M.L., V.E. and R.W.; methodology, M.L., S.G., N.L., S.Z., V.E. and R.W.; validation, M.L., V.E. and R.W.; formal analysis, M.L., V.E. and R.W.; investigation, M.L.; writing—original draft preparation, M.L., V.E. and R.W.; writing—review and editing, S.G., S.Z., V.E. and R.W.; visualization, M.L.; supervision, N.L., V.E. and R.W. All authors have read and agreed to the published version of the manuscript.

Funding: The work was supported by the Open Access Publishing Fund of Leipzig University, supported by the German Research Foundation within the program Open Access Publication Funding.

Institutional Review Board Statement: Not applicable.

Informed Consent Statement: Not applicable.

Data Availability Statement: Data are contained within the article or Supplementary Material.

Conflicts of Interest: The authors declare no conflict of interest.

References

1. WHO. *Antimicrobial Resistance—Global Report on Surveillance 2014*; World Health Organization: Geneva, Switzerland, 2014.
2. Lübbert, C.; Baars, C.; Dayakar, A.; Lippmann, N.; Rodloff, A.C.; Kinzig, M.; Sörgel, F. Environmental Pollution with Antimicrobial Agents from Bulk Drug Manufacturing Industries in Hyderabad, South India, Is Associated with Dissemination of Extended-Spectrum Beta-Lactamase and Carbapenemase-Producing Pathogens. *Infection* **2017**, *45*, 479–491. [[CrossRef](#)] [[PubMed](#)]
3. Wainwright, M.; Maisch, T.; Nonell, S.; Plaetzer, K.; Almeida, A.; Tegos, G.P.; Hamblin, M.R. Photoantimicrobials—Are We Afraid of the Light? *Lancet Infect. Dis.* **2017**, *17*, e49–e55. [[CrossRef](#)]

4. Abrahamse, H.; Hamblin, M.R. New Photosensitizers for Photodynamic Therapy. *Biochem. J.* **2016**, *473*, 347–364. [[CrossRef](#)] [[PubMed](#)]
5. Amos-Tautua, B.M.; Songca, S.P.; Oluwafemi, O.S. Application of Porphyrins in Antibacterial Photodynamic Therapy. *Molecules* **2019**, *24*, 2456. [[CrossRef](#)]
6. Ezzeddine, R.; Al-Banaw, A.; Tovmasyan, A.; Craik, J.D.; Batinic-Haberle, I.; Benov, L.T. Effect of Molecular Characteristics on Cellular Uptake, Subcellular Localization, and Phototoxicity of Zn(II) N-Alkylpyridylporphyrins. *J. Biol. Chem.* **2013**, *288*, 36579–36588. [[CrossRef](#)]
7. Hamblin, M.R. Antimicrobial Photodynamic Inactivation: A Bright New Technique to Kill Resistant Microbes. *Curr. Opin. Microbiol.* **2016**, *33*, 67–73. [[CrossRef](#)]
8. Ragàs, X.; He, X.; Agut, M.; Roxo-Rosa, M.; Gonsalves, A.R.; Serra, A.C.; Nonell, S. Singlet Oxygen in Antimicrobial Photodynamic Therapy: Photosensitizer-Dependent Production and Decay in E. Coli. *Molecules* **2013**, *18*, 2712–2725. [[CrossRef](#)]
9. Ergaieg, K.; Chevanne, M.; Cillard, J.; Seux, R. Involvement of Both Type I and Type II Mechanisms in Gram-Positive and Gram-Negative Bacteria Photosensitization by a Meso-Substituted Cationic Porphyrin. *Sol. Energy* **2008**, *82*, 1107–1117. [[CrossRef](#)]
10. Gao, Y.; Mai, B.; Wang, A.; Li, M.; Wang, X.; Zhang, K.; Liu, Q.; Wei, S.; Wang, P. Antimicrobial Properties of a New Type of Photosensitizer Derived from Phthalocyanine against Planktonic and Biofilm Forms of Staphylococcus Aureus. *Photodiagnosis Photodyn. Ther.* **2018**, *21*, 316–326. [[CrossRef](#)]
11. Imlay, J.A. Pathways of Oxidative Damage. *Annu. Rev. Microbiol.* **2003**, *57*, 395–418. [[CrossRef](#)]
12. Wang, J.; Wu, H.; Yang, Y.; Yan, R.; Zhao, Y.; Wang, Y.; Chen, A.; Shao, S.; Jiang, P.; Li, Y.-Q. Bacterial Species-Identifiable Magnetic Nanosystems for Early Sepsis Diagnosis and Extracorporeal Photodynamic Blood Disinfection. *Nanoscale* **2017**, *10*, 132–141. [[CrossRef](#)]
13. Martinez De Pinillos Bayona, A.; Mroz, P.; Thunshelle, C.; Hamblin, M.R. Design Features for Optimization of Tetrapyrrole Macrocycles as Antimicrobial and Anticancer Photosensitizers. *Chem. Biol. Drug Des.* **2017**, *89*, 192–206. [[CrossRef](#)] [[PubMed](#)]
14. Cormick, M.P.; Quiroga, E.D.; Bertolotti, S.G.; Alvarez, M.G.; Durantini, E.N. Mechanistic Insight of the Photodynamic Effect Induced by Tri- and Tetra-Cationic Porphyrins on Candida Albicans Cells. *Photochem. Photobiol. Sci.* **2011**, *10*, 1556–1561. [[CrossRef](#)] [[PubMed](#)]
15. Salmon-Divon, M.; Nitzan, Y.; Malik, Z. Mechanistic Aspects of Escherichia Coli Photodynamic Inactivation by Cationic Tetra-Meso(N-Methylpyridyl)Porphine. *Photochem. Photobiol. Sci.* **2004**, *3*, 423–429. [[CrossRef](#)]
16. Tavares, A.; Dias, S.R.S.; Carvalho, C.M.B.; Faustino, M.A.F.; Tomé, J.P.C.; Neves, M.G.P.M.S.; Tomé, A.C.; Cavaleiro, J.A.S.; Cunha, Â.; Gomes, N.C.M.; et al. Mechanisms of Photodynamic Inactivation of a Gram-Negative Recombinant Bioluminescent Bacterium by Cationic Porphyrins. *Photochem. Photobiol. Sci.* **2011**, *10*, 1659–1669. [[CrossRef](#)] [[PubMed](#)]
17. Zhao, Z.-J.; Xu, Z.-P.; Ma, Y.-Y.; Ma, J.-D.; Hong, G. Photodynamic Antimicrobial Chemotherapy in Mice with Pseudomonas Aeruginosa-Infected Wounds. *PLoS ONE* **2020**, *15*, e0237851. [[CrossRef](#)]
18. Almeida, P.P.; Pereira, Í.S.; Rodrigues, K.B.; Leal, L.S.; Marques, A.S.; Rosa, L.P.; da Silva, F.C.; da Silva, R.A.A. Photodynamic Therapy Controls of Staphylococcus Aureus Intradermal Infection in Mice. *Lasers Med. Sci.* **2017**, *32*, 1337–1342. [[CrossRef](#)]
19. Branco, T.M.; Valério, N.C.; Jesus, V.I.R.; Dias, C.J.; Neves, M.G.P.M.S.; Faustino, M.A.F.; Almeida, A. Single and Combined Effects of Photodynamic Therapy and Antibiotics to Inactivate Staphylococcus Aureus on Skin. *Photodiagnosis Photodyn. Ther.* **2018**, *21*, 285–293. [[CrossRef](#)]
20. Wiegand, I.; Hilpert, K.; Hancock, R.E.W. Agar and Broth Dilution Methods to Determine the Minimal Inhibitory Concentration (MIC) of Antimicrobial Substances. *Nat. Protoc.* **2008**, *3*, 163–175. [[CrossRef](#)]
21. McCarthy, J.A.; Thomas, H.A.; Delaney, J.E. Evaluation of the Reliability of Coliform Density Tests. *Am. J. Public Health Nations Health* **1958**, *48*, 1628–1635. [[CrossRef](#)]
22. Pazos-Perez, N.; Pazos, E.; Catala, C.; Mir-Simon, B.; Gómez-de Pedro, S.; Sagales, J.; Villanueva, C.; Vila, J.; Soriano, A.; García de Abajo, F.J.; et al. Ultrasensitive Multiplex Optical Quantification of Bacteria in Large Samples of Biofluids. *Sci. Rep.* **2016**, *6*, 29014. [[CrossRef](#)] [[PubMed](#)]
23. Tsuji, H.; Matsuda, K.; Nomoto, K. Counting the Countless: Bacterial Quantification by Targeting rRNA Molecules to Explore the Human Gut Microbiota in Health and Disease. *Front. Microbiol.* **2018**, *9*, 1417. [[CrossRef](#)] [[PubMed](#)]
24. Marques, S.M.; Esteves da Silva, J.C.G. Firefly Bioluminescence: A Mechanistic Approach of Luciferase Catalyzed Reactions. *IUBMB Life* **2009**, *61*, 6–17. [[CrossRef](#)] [[PubMed](#)]
25. Tannous, B.A. Gaussia Luciferase Reporter Assay for Monitoring Biological Processes in Culture and in Vivo. *Nat. Protoc.* **2009**, *4*, 582–591. [[CrossRef](#)] [[PubMed](#)]
26. Dingle, T.C.; Butler-Wu, S.M. Maldi-ToF Mass Spectrometry for Microorganism Identification. *Clin. Lab. Med.* **2013**, *33*, 589–609. [[CrossRef](#)] [[PubMed](#)]
27. Schastak, S.; Jean, B.; Handzel, R.; Kostenich, G.; Hermann, R.; Sack, U.; Orenstein, A.; Wang, Y.-S.; Wiedemann, P. Improved Pharmacokinetics, Biodistribution and Necrosis in Vivo Using a New near Infra-Red Photosensitizer: Tetrahydroporphyrin Tetratosylat. *J. Photochem. Photobiol. B* **2005**, *78*, 203–213. [[CrossRef](#)] [[PubMed](#)]
28. Riyad, Y.M.; Naumov, S.; Schastak, S.; Griebel, J.; Kahnt, A.; Häupl, T.; Neuhaus, J.; Abel, B.; Hermann, R. Chemical Modification of a Tetrapyrrole-Type Photosensitizer: Tuning Application and Photochemical Action beyond the Singlet Oxygen Channel. *J. Phys. Chem. B* **2014**, *118*, 11646–11658. [[CrossRef](#)]

29. Habermann, N.; Wachs, M.; Schulz, S.; Werdehausen, R.; Schwarz, U.T. Development and Characterization of Planar LED Arrays for Medical Applications. *Jpn. J. Appl. Phys.* **2019**, *58*, SCCC25. [[CrossRef](#)]
30. Beirão, S.; Fernandes, S.; Coelho, J.; Faustino, M.A.F.; Tomé, J.P.C.; Neves, M.G.P.M.S.; Tomé, A.C.; Almeida, A.; Cunha, A. Photodynamic Inactivation of Bacterial and Yeast Biofilms With a Cationic Porphyrin. *Photochem. Photobiol.* **2014**, *90*, 1387–1396. [[CrossRef](#)]
31. Prasanth, C.S.; Karunakaran, S.C.; Paul, A.K.; Kussovski, V.; Mantareva, V.; Ramaiah, D.; Selvaraj, L.; Angelov, I.; Avramov, L.; Nandakumar, K.; et al. Antimicrobial Photodynamic Efficiency of Novel Cationic Porphyrins towards Periodontal Gram-Positive and Gram-Negative Pathogenic Bacteria. *Photochem. Photobiol.* **2014**, *90*, 628–640. [[CrossRef](#)]
32. Ziganshyna, S.; Guttenberger, A.; Lippmann, N.; Schulz, S.; Bercker, S.; Kahnt, A.; Rüffer, T.; Voigt, A.; Gerlach, K.; Werdehausen, R. Tetrahydroporphyrin-Tetratosylate (THPTS)-Based Photodynamic Inactivation of Critical Multidrug-Resistant Bacteria in Vitro. *Int. J. Antimicrob. Agents* **2020**, *55*, 105976. [[CrossRef](#)] [[PubMed](#)]
33. Magiorakos, A.-P.; Srinivasan, A.; Carey, R.B.; Carmeli, Y.; Falagas, M.E.; Giske, C.G.; Harbarth, S.; Hindler, J.F.; Kahlmeter, G.; Olsson-Liljequist, B.; et al. Multidrug-Resistant, Extensively Drug-Resistant and Pandrug-Resistant Bacteria: An International Expert Proposal for Interim Standard Definitions for Acquired Resistance. *Clin. Microbiol. Infect.* **2012**, *18*, 268–281. [[CrossRef](#)]
34. Glass, S.; Kühnert, M.; Lippmann, N.; Zimmer, J.; Werdehausen, R.; Abel, B.; Eulenburger, V.; Schulze, A. Photosensitizer-Loaded Hydrogels for Photodynamic Inactivation of Multiresistant Bacteria in Wounds. *RSC Adv.* **2021**, *11*, 7600–7609. [[CrossRef](#)] [[PubMed](#)]
35. Cox, C.D.; Adams, P. Siderophore Activity of Pyoverdinin for *Pseudomonas Aeruginosa*. *Infect. Immun.* **1985**, *48*, 130–138. [[CrossRef](#)] [[PubMed](#)]
36. Kramer, B.; Wunderlich, J.; Muranyi, P. ATP-Synthesis Capacity of Pulsed Light-Exposed Bacteria. *Syst. Appl. Microbiol.* **2017**, *40*, 383–387. [[CrossRef](#)] [[PubMed](#)]
37. Al-Mutairi, R.; Tovmasyan, A.; Batinic-Haberle, I.; Benov, L. Sublethal Photodynamic Treatment Does Not Lead to Development of Resistance. *Front. Microbiol.* **2018**, *9*, 1699. [[CrossRef](#)]
38. Kakihana, Y.; Cheng, L.; Fang, L.-F.; Wang, S.-Y.; Jeon, S.; Saeki, D.; Rajabzadeh, S.; Matsuyama, H. Preparation of Positively Charged PVDF Membranes with Improved Antibacterial Activity by Blending Modification: Effect of Change in Membrane Surface Material Properties. *Colloids Surf. A Physicochem. Eng. Asp.* **2017**, *533*, 133–139. [[CrossRef](#)]
39. Knauf, G.A.; Cunningham, A.L.; Kazi, M.I.; Riddington, I.M.; Crofts, A.A.; Cattoir, V.; Trent, M.S.; Davies, B.W. Exploring the Antimicrobial Action of Quaternary Amines against *Acinetobacter Baumannii*. *mBio* **2018**, *9*, e02394–e02417. [[CrossRef](#)]
40. Hoque, J.; Adhikary, U.; Yadav, V.; Samaddar, S.; Konai, M.M.; Prakash, R.G.; Paramanandham, K.; Shome, B.R.; Sanyal, K.; Haldar, J. Chitosan Derivatives Active against Multidrug-Resistant Bacteria and Pathogenic Fungi: In Vivo Evaluation as Topical Antimicrobials. *Mol. Pharm.* **2016**, *13*, 3578–3589. [[CrossRef](#)]
41. Yao, F.; Fu, G.-D.; Zhao, J.; Kang, E.-T.; Neoh, K.G. Antibacterial Effect of Surface-Functionalized Polypropylene Hollow Fiber Membrane from Surface-Initiated Atom Transfer Radical Polymerization. *J. Membr. Sci.* **2008**, *319*, 149–157. [[CrossRef](#)]
42. Sułek, A.; Pucelik, B.; Kobielski, M.; Barzowska, A.; Dąbrowski, J.M. Photodynamic Inactivation of Bacteria with Porphyrin Derivatives: Effect of Charge, Lipophilicity, ROS Generation, and Cellular Uptake on Their Biological Activity In Vitro. *Int. J. Mol. Sci.* **2020**, *21*, 8716. [[CrossRef](#)] [[PubMed](#)]
43. Faraj Tabrizi, P.; Wennige, S.; Berneburg, M.; Maisch, T. Susceptibility of SodA- and SodB-Deficient *Escherichia Coli* Mutant towards Antimicrobial Photodynamic Inactivation via the Type I-Mechanism of Action. *Photochem. Photobiol. Sci.* **2018**, *17*, 352–362. [[CrossRef](#)] [[PubMed](#)]
44. Tegos, G.P.; Masago, K.; Aziz, F.; Higginbotham, A.; Stermitz, F.R.; Hamblin, M.R. Inhibitors of Bacterial Multidrug Efflux Pumps Potentiate Antimicrobial Photoinactivation. *Antimicrob. Agents Chemother.* **2008**, *52*, 3202–3209. [[CrossRef](#)] [[PubMed](#)]
45. Berndt-Paetz, M.; Schulze, P.; Stenglein, P.C.; Weimann, A.; Wang, Q.; Horn, L.-C.; Riyad, Y.M.; Griebel, J.; Hermann, R.; Glasow, A.; et al. Reduction of Muscle-Invasive Tumors by Photodynamic Therapy with Tetrahydroporphyrin-Tetratosylate in an Orthotopic Rat Bladder Cancer Model. *Mol. Cancer Ther.* **2019**, *18*, 743–750. [[CrossRef](#)]
46. Berndt-Paetz, M.; Weimann, A.; Sieger, N.; Schastak, S.; Riyad, Y.M.; Griebel, J.; Arthanareeswaran, V.K.A.; Stolzenburg, J.-U.; Neuhaus, J. Tetrahydroporphyrin-Tetratosylate (THPTS): A near-Infrared Photosensitizer for Targeted and Efficient Photodynamic Therapy (PDT) of Human Bladder Carcinoma. An in Vitro Study. *Photodiagnosis Photodyn. Ther.* **2017**, *18*, 244–251. [[CrossRef](#)]
47. Walther, J.; Schastak, S.; Dukic-Stefanovic, S.; Wiedemann, P.; Neuhaus, J.; Claudepierre, T. Efficient Photodynamic Therapy on Human Retinoblastoma Cell Lines. *PLoS ONE* **2014**, *9*, e87453. [[CrossRef](#)]